Laser intensity dependence of femtosecond near-infrared optoinjection

Cheng Peng,[1] Robert E. Palazzo,[2] and Ingrid Wilke[1]
[1]*Department of Physics, Applied Physics & Astronomy, Rensselaer Polytechnic Institute, 110 8th Street, Troy, New York 12180, USA*
[2]*Department of Biology and Center for Biotechnology and Interdisciplinary Research, Rensselaer Polytechnic Institute, Wadsworth Center NY State Department of Health, 110 8th Street, Troy, NY 12180, USA and The Marine Biological Laboratory, Woodshole, Massachusetts 02543, USA*
(Received 2 March 2006; revised manuscript received 13 December 2006; published 3 April 2007)

We report an experimental study on transient membrane permeabilization of single living bovine aortic endothelial cells (BAEC) by tightly focused femtosecond near-infrared laser pulses. The membrane permeabilization of the BAEC cells was studied as a function of the incident laser intensity. The rate of dye uptake by the cells was analyzed using time-lapse imaging. We found that membrane permeabilization occurs for laser intensities higher than 4.0×10^{12} W/cm^2. For laser intensity above 3.3×10^{13} W/cm^2 the cell disintegrates. Within these two limits the rate of dye uptake increases logarithmically with increasing laser intensity. This functional dependence is explained by considering the Gaussian intensity distribution across the laser focal spot. Cell membrane permeabilization is explained by the creation of a plasma within the laser focal spot. The physical understanding of the relationship between dye uptake, pore characteristics, and laser intensity allows control of the concentrations of molecules delivered into cells through the control of pore characteristics.

DOI: 10.1103/PhysRevE.75.041903 PACS number(s): 47.63.mh, 87.80.−y, 87.64.−t, 87.90.+y

INTRODUCTION

The plasma membrane of a cell constitutes a major barrier for the entry of extrinsic molecules into the cell interior. Selective and reversible permeabilization of this barrier is a prerequisite for many biotechnological applications [1]. Several methods of cell permeabilization are based on the application of physical force, which include microinjection by glass pipettes [2], electroporation [3,4], biolistics [5], and microinjection by laser beams [6]. Although physical methods are destructive by nature, they have certain advantages over biological and chemical methods for membrane permeabilization. First they can be efficiently applied to a broad spectrum of cell types because physical forces function based on universal physical principles. Second, the control of the intensity and duration of the physical force can provide significant control of the process of permeabilization. Furthermore, physical methods usually result only in a minor, localized, and transient disturbance on the rest of the cell compared to chemical methods. Physical methods have been well developed within the past two decades and are widely used in biological and medical research. However, current methods have some major drawbacks. For example, microinjection by glass pipettes is characterized by low cell viability and low transfection efficiency, and is limited by cell size and type. Electroporation and biolistics cannot provide quantitative control over the amount of materials delivered into the cells or are difficult to apply to a single cell. Microinjection by lasers in the UV or the visible spectral range raises concerns about major damage to the cell membrane and the cell, even cytogenetic damage due to the strong absorption by certain cellular constituents such as nucleic acid in the UV and the visible spectral range [6–10].

Recently, a new method for microinjection, which employs femtosecond (fs) near-infrared (nir) laser pulses to create transient pores in cell membranes has been reported [11]. Koenig *et al.* reported the targeted transportation of plasmid DNA vector pEGFP-N1 encoding enhanced green fluorescent protein (EGFP) into Chinese hamster ovarian (CHO) and rat-kangaroo kidney epithelial (PtK2) cells by the femtosecond 800 nm laser. They observed 100% transfection efficiency and no detrimental effects on growth and division. Mohanty *et al.* [12] also performed the injection of impermeable dyes (propidium iodide and merocyanine 540) and a plasmid (pEGFP-N1) encoding green fluorescent protein (GFP) into human breast adenocarcinoma cells (MCF-7) using a nanosecond pulsed 1064 nm laser. They also observed that cell membrane integrity and viability were fully preserved. This work demonstrates that optoinjection by fs nir laser pulses is a promising new tool for loading cells with extrinsic molecules. The previous work on fs nir optoinjection of single living cells has been mainly focused on the biological response of the cells to fs nir laser pulses while the relationship between cell permeability and laser pulse characteristics remains unexplored. In this paper, we present an experimental study on fs nir optoinjection of membrane impermeable fluorescent dyes in bovine aortic endothelial cells (BAEC). In particular, we focus on the investigation of pore creation and dye uptake as a function of the incident laser intensity. The objective is to achieve a quantitative understanding of the rate of dye uptake by the cell dependent on the incident laser intensity. This knowledge will enable the controlled delivery of molecules by fs nir optoinjection into a target cell by adjusting the incident laser intensity.

MATERIALS AND METHODS

Cell culture. BAECs were obtained from VecTechnologies (Rensselaer, NY). Cells were cultured in Dulbecco's modified Eagle's medium from Gibco (Carlsbad, CA), supplemented with 10% calf serum, 1% *L*-glutamine, 1% antibody, (Penicilin-streptomyrin) and 2.5% Hepes buffer solution. For

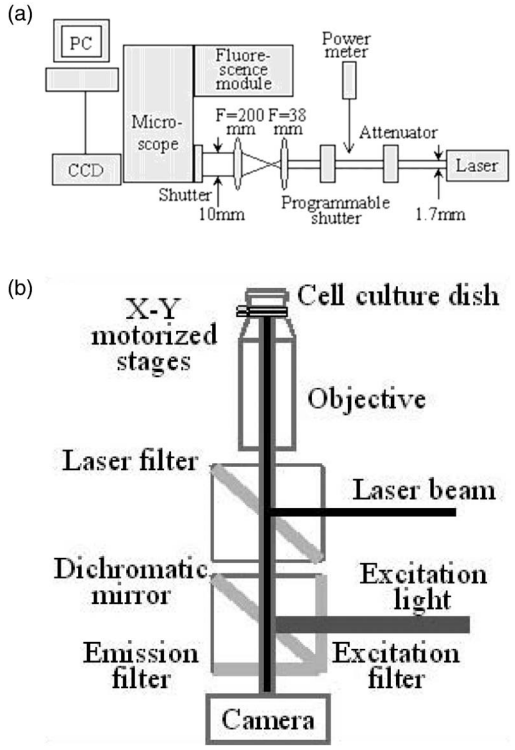

FIG. 1. (a) Schematic of optical setup. The femtosecond near-infrared laser is coupled into the laser port of an inverted fluorescence microscope. The laser beam diameter is expanded from 1.7 to 10 mm by two lenses with focal length $f=38$ mm and $f=200$ mm, respectively. The laser power is controlled by a variable attenuator and measured by a laser power meter. The exposure time of the cell samples to the laser beam is controlled by a programmable shutter. The experiment is observed by a video camera. Images are stored on a personal computer. (b) Schematic of the laser beam path inside the inverted fluorescence microscope. A dichroic mirror (laser filter) in the upper filter wheel directs the laser beam through the objective onto the cell sample. The filter cubes for the fluorescence microscopy are in the lower filter wheel.

optoinjection experiments BAEC cells were rinsed twice in phosphate buffered saline (PBS) (Gibco, Carlsbad, CA) and 1 ml of BAEC cells in PBS solution was placed in a 35 mm glass-bottomed cell culture dish (MatTek corporation, Ashland, MA). For dye uptake experiments 100 μl of 45 m Mol/1 Lucifer yellow (Molecular Probes, Carlsbad, CA) stock solution or 5 μl of 5 mg/ml propidium iodide (Molecular Probes, Carlsbad, CA) were added to the BAEC cells cultured in 1 ml PBS of suspension prior to laser exposure.

Laser setup. A spectra physics (Irvine, CA) tsunami femtosecond near-infrared laser beam (130 fs laser pulse duration, 82 MHz laser pulse repetition rate, 800 nm wavelength, TEM_{00} mode) was directed through the laser port of a Nikon TE2000 inverted fluorescence microscope (Nikon, Japan) as shown in Figs. 1(a) and 1(b). A dichroic mirror in the upper filter wheel was used to direct the laser light through a Nikon Cfi Plan Fluor ×40 1.30 NA oil objective. The laser beam diameter was expanded from 1.7–10 mm prior to entering the microscope by two 1″ diameter plan-convex lenses of

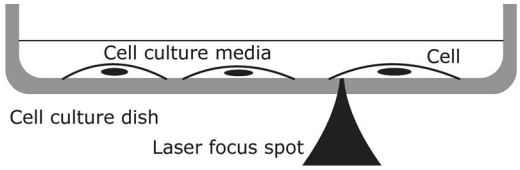

FIG. 2. Illustration of the principle of dye uptake experiments. Cells are cultured in media containing membrane impermeable fluorescent dyes. The laser focal spot is directed onto the cell membrane. Cell membrane permeabilization by the laser beam is probed by observing dye uptake by the cell.

focal lengths 38 and 200 mm, respectively. The laser power was controlled by a variable laser beam attenuator from Edmund Scientific (Barrington, NJ). The exposure time of the targeted cell was controlled by a programmable mechanical shutter by Uniblitz Electronic (Vincent Associates, Rochester, NY). The laser power, wavelength, and laser pulse duration were measured by Melles Griot (Carlsbad, CA) 13PEM001 laser power meter, Ocean Optics (Dunedin, FL) UBS2000 optical spectrometer, and a femtosecond autocorrelator.

Fluorescence microscopy and image processing. The dye uptake by the BAEC cells during and after optoinjection (Fig. 2) was observed through a Nikon TE2000 inverted fluorescence microscope with a Nikon Cfi Plan Fluor ×40 1.30 N.A. oil objective. For Lucifer Yellow uptake studies a Lucifer Yellow filter cube from Chroma (Rockingham, VT) was used. For PI uptake studies a 96313 C-FL Y-2E/C Texas Red filter cube (Chroma, Rockingham, VT) was used. For this filter cube the excitation filter wavelengths are 540–580 nanometers (bandpass, 560 CWL), the dichromatic mirror cut-on wavelength is 595 nanometers (longpass, LP) and the barrier filter wavelengths are 600–660 nanometers (bandpass, 630 CWL). Images were captured by a Roper Scientific (Tucson, AZ) Coolsnap HQ ccd camera and processed by Universal Imaging Metavue (Downingtown, PA) software on a computer.

Protocol of transient pore creation. The cell culture dish containing BAEC cells was brought in contact with a ×40 oil objective until the image of the cells was clearly seen on the computer screen. In order to determine the position of the laser focal spot in the field of view of the microscope the laser power was reduced to a low level by rotating the laser beam attenuator. Next, the laser beam was introduced to the microscope by opening the programmable mechanical shutter in the laser beam path and the laser port shutter of the microscope. The laser beam was then focused on the bottom of the cell culture dish. An image of the laser focal spot was seen on the pc monitor. The position of the laser focal spot on the pc monitor was marked by the cursor and the programmable mechanical shutter was closed again. The targeted cell and the desired location on the cell for the creation of an artificial pore were moved to the position of the laser focal spot by moving the microscope stage. The alignment of the laser beam and cell is observed through the video camera on the pc monitor. We focus the laser beam on the cell membrane by adjusting the z dimension such that we observe simultaneously a sharp image of the laser focus and the cell

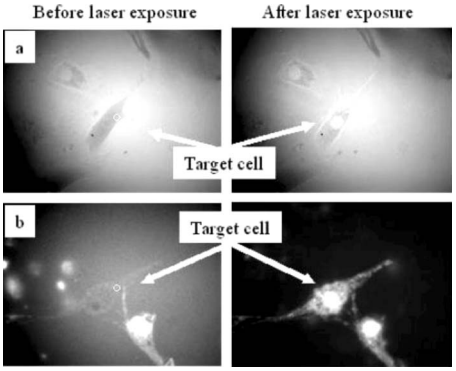

FIG. 3. (a) Left: The picture shows a BAEC cell before laser exposure in the presence of Lucifer Yellow. The laser focal spot is marked by the white circle. (a) Right: The picture shows BAEC cells after laser exposure in the presence of Lucifer Yellow. After laser exposure fluorescence is observed inside the BAEC cell. (b) The same experiment has been performed with PI as fluorescent probe. Again the location of the laser focal spot is indicated by a white circle. Again, after laser exposure fluorescence is observed inside the cell.

surface on the pc monitor. The desired laser power for pore creation was selected by rotating the laser beam attenuator and was measured by the laser power meter. The laser exposure time of the cell was selected by programming open duration, delay, and repetition intervals of the mechanical shutter. For observations of dye uptake the appropriate filter wheel was turned in place. Time-lapse video imaging of dye uptake was preset by selecting the frame rate and recording duration using Metavue software. The transient pore creation and its observation were initiated by simultaneously starting the preset shutter program and the time-lapse imaging. This started the exposure of the target location on the cell membrane to the focused laser beam and the video imaging of dye uptake. The laser exposure ended when the shutter was closed after the preset shutter open time had elapsed.

Time-lapse analysis of dye uptake. Time-lapse analysis was performed by selecting the corresponding option using Metavue software. The desired region for analysis inside the cell was selected by using the cursor on the screen. The temporal development of the fluorescence intensity in the selected region was extracted from the time-lapse record using the region measurement routine. The data was saved to an ASC file and further analyzed using ORIGIN software.

RESULTS AND DISCUSSIONS

Results of our dye uptake experiments with BAEC cells and fluorescent probes Lucifer Yellow and propidium iodide are displayed in Fig. 3. Figure 3(a) (left) shows a BAEC cell before laser exposure in the presence of Lucifer Yellow. The position of the laser focal spot is marked by the white circle. Figure 3(a) (right) shows BAEC cells after laser exposure in the presence of Lucifer Yellow (LY). Fluorescence is observed inside the BAEC cell. The same experiment has been performed with PI as fluorescent probe [Fig. 3(b)]. Again the location of the laser focal spot is indicated by a white circle. After laser exposure fluorescence is observed inside the cell. The behavior of the dyes in the cells is as expected. PI mainly accumulates in the nucleus. LY, as a nonreactive dye, fills the whole interior of the cell. In order to verify that laser exposure and the interaction of the laser beam with the cell membrane is the cause of change in membrane permeability several control experiments were performed. Accordingly, we did not observe dye uptake by the BAEC cells when the cells were not exposed to the laser beam. Also, we did not observe dye uptake when the laser focus was in the vicinity of the cell but not on the cell. Moreover, we did not observe an increase of fluorescence inside the cell when the cell was exposed to the focused laser beam but no dye was present in the cell culture medium. From the observations illustrated in Fig. 3 and the results of the control experiments we conclude that the focused fs nir laser beam creates an artificial pore or pores in the cell membrane.

In order to achieve a quantitative understanding of cell membrane permeabilization by fs nir optoinjection we studied dye uptake by BAEC cells as a function of the incident peak laser intensity $I_i = P/(\nu_L \tau \pi r_L^2)$. The laser intensity I_i is determined by the laser pulse duration τ, the laser pulse repetition rate ν_L, the incident laser power P, and the laser focal spot πr_L^2 with $2r_L$ the laser focal spot diameter. For experiments the laser intensity was varied by keeping the laser pulse duration, the laser pulse repetition rate, and the laser focal spot diameter fixed while the incident laser power was varied between 0 and 400 mW. The effective laser pulse duration at the sample was estimated to be $\tau \approx 200$ fs by considering the group-velocity dispersion induced by the microscope objective [13]. A laser focal spot diameter $2r_L = \lambda/(2\ \mathrm{NA}) = 308$ nm was calculated from the laser wavelength $\lambda = 800$ nm and the numerical aperture of the microscope objective NA=1.30 assuming geometrical optics [24].

Quantitative analysis of dye uptake was performed by analyzing time-lapse video records of the dye uptake experiments. An example of a time-lapse record of dye uptake under laser exposure is illustrated in Fig. 4. The region for time-lapse analysis of the exposed cell was selected by using the cursor on the screen. We observed that the fluorescence intensity emitted from a selected region inside the cell starts to increase when the laser shutter is opened ($t=18$ s) and the cell is exposed to the tightly focused laser beam. During laser exposure the fluorescence intensity from the selected region increases linearly with time until $t=38$ s (Fig. 4). After the laser shutter is closed we observe a further sublinear increase of the fluorescence intensity until the fluorescence intensity measured in the selected region reaches a constant value at time $t=240$ s. We interpret the linear increase in fluorescence intensity in the selected region inside the cell during laser exposure as a measure of the number N of dye molecules diffusing into the cell through the transient pore created by the fs nir laser beam. The sublinear increase of the fluorescence intensity in the selected region inside the cell after laser exposure is attributed to the time required for complete pore resealing and the time required for the dye molecules to diffuse from the location of the pore to the selected region in the cell. The modeling of the diffusive flow of molecules into the cell through the laser-induced pore(s) as well as the diffusive flow within the cell is a work

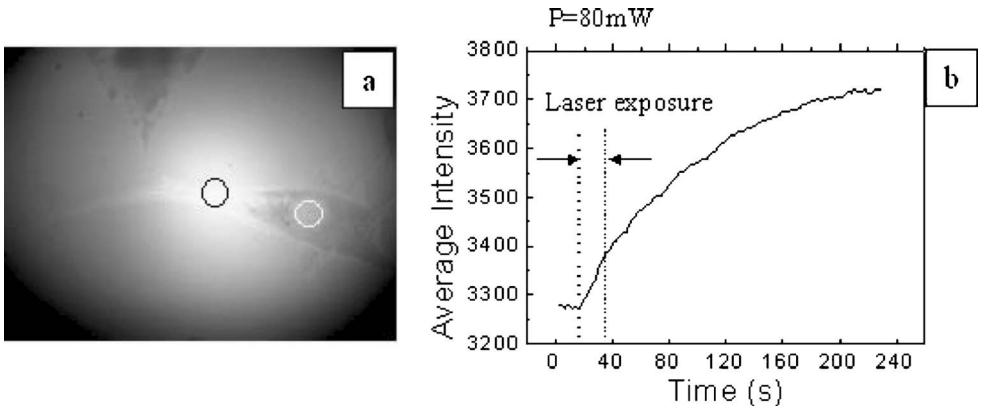

FIG. 4. (a) Target BAEC cell after optoinjection. The location of the laser focal spot is indicated by a black circle. The region selected for time-lapse analysis is indicated by a white circle. The illumination sites and the observation sites are always in constant distance. (b) Time-lapse analysis of dye (Lucifer Yellow) uptake process. The fluorescence intensity emitted by the selected region inside the cell starts to increase when the laser shutter is opened at time $t=18$ s and the cell is exposed to the beam. During laser exposure the fluorescence intensity from the selected region increases linearly with time. After the laser shutter is closed at time $t=38$ s a further sublinear increase of the fluorescence intensity is observed until the fluorescence intensity measured in the selected region reaches a constant value at time $t=240$ s. The laser intensity was 6.4×10^{12} W/cm^2. The linear increase in fluorescence intensity in the selected region inside the cell during laser exposure is a measure of the number of dye molecules diffusing into the cell through the transient pore created by the fs nir laser beam. The linear slope of the time-lapse record during laser exposure is the rate of the diffusive flow $\Phi \sim dN/dt$ of dye molecules into the cell.

in progress. Results of the modeling will be discussed elsewhere.

LASER INTENSITY DEPENDENCE OF DYE UPTAKE

Further discussions now focus on the rate of increase of the fluorescence intensity during laser exposure. We interpret the slope of the time-lapse record during laser exposure as the rate of the diffusive flow $\Phi \propto dN/dt$ of dye molecules into the cell. In order to investigate the relationship between laser intensity, pore creation, and dye uptake we analyzed the time-lapse records of approximately 200 dye uptake optoinjection experiments performed at different laser intensities and determined the rate of increase of the fluorescence intensity Φ for each experiment. The results of these experiments and the analysis are illustrated in Fig. 5. As illustrated in Fig. 5 no dye uptake by the cell was observed for laser intensities less than 4.0×10^{12} W/cm^2. For laser intensities between 4.0×10^{12} W/cm^2 and 1.0×10^{13} W/cm^2 dye uptake by the cells was observed. In this intensity range the flow of dye molecules into the cells increases monotonically with increasing laser intensities. The cell-to-cell variations in the rate of dye uptake are indicated by the error bars. For laser intensities above 1.0×10^{13} W/cm^2 and less than 3.3×10^{13} W/cm^2 the flow of dye molecules into the cell no longer increases with increasing laser intensities and the cell-to-cell variations in dye uptake strongly increase. Above 3.3×10^{13} W/cm^2 cells disintegrate with a very high probability when exposed to the laser beam. If we consider the dye uptake by the cells in dependence of the energy per laser pulse$E$ and energy density j_E, characteristic values densities for the observations illustrated in Fig. 5 are 0.6, 1.8, and 4.9 nJ, and 0.8, 2.4, and 6.5 J/cm^2, respectively. The laser pulse energy E is calculated from the incident laser power P and the laser pulse repetition rate ν_L as $E=P/\nu_L$. The energy density j_E obtained by dividing the laser pulse energy by the laser focal spot is πr_L^2.

During fs nir optoinjection a single cell is exposed to the laser focus. Generally, we observed that almost all cells ($\sim$100%) exhibited dye uptake after laser exposure for laser intensities higher than 4.0×10^{12} W/cm^2. Similarly, we observed that almost no cells exhibited dye uptake after laser exposure for laser intensities less than 4.0×10^{12} W/cm^2. Cell viability of BAEC cells after laser exposure was examined using Calcein AM. These experiments demonstrated that cell viability of BAEC cells is preserved during femtosecond near-infrared optoinjection for laser intensities lower than 1.2×10^{13} W/cm^2. The results of the cell viability studies will be published elsewhere.

In our experiments, we also observed the formation of vapor bubbles in the laser focal spot during laser exposure. The formation of a vapor bubble was a statistical event with the probability of vapor bubble formation dependent on laser intensity. The probability of generating a vapor bubble is 0% for laser intensities $\leq6.5\times10^{12}$ W/cm^2. For laser intensities between 8.1×10^{12} W/cm^2 and 1.2×10^{13} W/cm^2 the probability for vapor bubble generation increases up to 50% and for laser intensities between 2.8×10^{12} W/cm^2 to 3.2×10^{12} W/cm^2 vapor bubbles occur with 60–100% probability during laser exposure. The vapor bubble diameters range from 5 to 20 μm. Generally, we observe that vapor bubble formation induces cell morphology changes. The morphology change is more severe for higher laser intensities. We observe for laser intensities higher than 3.2×10^{13} W/cm^2 that bubble formation results in the destruction of the treated cell. The destruction manifests itself in strong morphology changes (cell "explodes" or cell curls up from the bottom of the cell culture dish). For intermediate laser intensities ($\sim1.2\times10^{13}$–3×10^{13} W/cm^2 we observe sometimes but not always smaller morphology changes of the cell near the laser focus such as the small movement of cell organelles

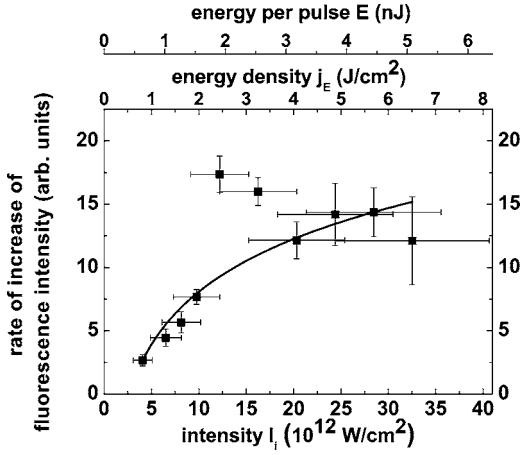

FIG. 5. The graph shows the rate of increase of average fluorescent intensity under different laser intensities in optoinjection experiment performed with BAEC and Lucifer Yellow. The rate of increase of fluorescence intensity is the linear slope of the time-lapse records during laser exposure (Fig. 4). The linear slope of time-lapse records during laser exposure are rates of diffusive flow $\Phi \sim dN/dt$ of dye molecules into the cell. We have performed optoinjection experiments on living BAEC at ten different laser intensities I_i. Furthermore, we have performed optoinjection experiments on 20 individual cells for a given laser intensity I_i. The total number of BAEC cells investigated in our study was 200 BAEC cells. For each individual cell, the rate of increase of fluorescence intensity was determined from the corresponding time-lapse record. The data points displayed are the statistical means of the rate of increase of fluorescence intensity observed for 20 living cells investigated at that laser intensity I_i. The vertical error bars are the standard error of the mean rate of increase of fluorescence intensity. The statistical analysis was performed using the descriptive statistics software package in the data analysis software ORIGIN 7.0. We do not observe dye uptake for laser intensity levels less than 4.0×10^{12} W/cm^2. For laser intensities between 4.0×10^{12} W/cm^2 and 1.0×10^{13} W/cm^2 we observe a controlled increase of the rate of dye uptake with increasing laser intensity. The vertical error bars indicate the cell-to-cell variations in rate of dye uptake for a given laser intensity. For laser intensities between 1.0×10^{13} W/cm^2 and 3.5×10^{13} W/cm^2 we observe larger cell-to-cell variations than for laser intensities below 1.0×10^{13} W/cm^2. For laser power levels larger than 3.5×10^{13} W/cm^2 we observe disintegration of the cell. The solid line is a fit of $\Phi=A\ln(I_i/B)$ to the measured data with $A=6.02\pm1.13$ and $B=(2.62\pm0.87)\times10^{12}$ W/cm^2. This logarithmic dependence of Φ on I_i is derived assuming laser-induced plasma formation in the laser focal spot and considering the Gaussian intensity distribution in the laser focal spot.

(within the resolution of our microscope). As discussed earlier cell viability of BAEC cells is preserved during femtosecondnear-infrared optoinjection for laser intensities lower than 1.2×10^{13} W/cm^2.

Next, we discuss the laser intensity dependence of the rate of dye uptake by the cells within the models of laser-induced plasma formation and photodisruption [14]. When femtosecond laser pulses are tightly focused on a transparent media (such as mammalian cells at near-infrared wavelength), the intensity in the laser focal spot can become sufficiently high to induce a plasma consisting of free electrons and ions by multiphoton absorption and subsequent cascade ionization. Since multiphoton absorption is a strongly nonlinear process, plasma formation is confined to the laser focal volume. When the plasma density increases above a certain intensity threshold laser-induced breakdown (LIB) occurs. LIB is characterized by shock wave generation and cavitation bubble formation. From an experimental point of view, the threshold for plasma formation is the ablation of matter and for LIB the observation of shock waves or bubble formation. From a theoretical point of view, the probability threshold for laser-induced breakdown is defined by the generation of a free electron density larger than 10^{21} cm^{-3} [15].

As already described we observed three characteristic laser intensity thresholds at 4.0×10^{12}, 1.0×10^{13}, and 3.3×10^{13} W/cm^2 in our experiments. We attribute the first threshold at 4.0×10^{12} W/cm^2 to be the onset of plasma-induced ablation of the cell membrane in the laser focal spot. The second threshold at 1.0×10^{13} W/cm^2 is attributed to the onset of LIB breakdown. The third threshold at 6.5×10^{13} W/cm^2 is attributed to photodisruption of the entire cell due to the mechanical effects of the plasma. This interpretation is supported by the following arguments.

The 0.8 nJ energy threshold for dye uptake by BAEC cells in our experiment agrees well with the 1.0–1.7 nJ energy threshold for the ablation of subcellular material reported by Heisterkamp *et al.* [16]. Heisterkamp *et al.* investigated the laser pulse energy dependence of subcellular dissection in fixed bovine capillary endothelial cells by femtosecond nir laser pulses. Their experiments were performed under almost identical conditions as our measurements (790 nm laser wavelength, 200–250 fs pulse duration at the cell sample, 80 MHz repetition rate, 1.4 NA oil immersion objective, cell type). Our observed energy threshold for plasma-induced ablation is slightly lower than that reported by Heisterkamp *et al.* This is probably due to the fact that our dye uptake experiments involve Lucifer Yellow (molecule diameter 1.1 nm), which probes a smaller ablation width.

The energy density threshold of 0.8 J/cm^2 for dye uptake in our experiment also agrees very well with the results by Loesel *et al.* [17]. They observed the onset of plasma-induced ablation in bovine neural tissue for 100 fs laser pulses at 630 nm wavelength, 100 Hz repetition rate and 20 μm focal spot diameter for energy densities higher than 1.5 J/cm^2. The Loesel *et al.* experiments were performed at a shorter wavelength and with a larger laser focal spot diameter. Nevertheless, their results are comparable to those based on the theoretical work of Kennedy *et al.* [18], which predicts that the free electron density in the laser focal spot is independent of laser wavelength and the focal spot size for laser pulses shorter than a few picoseconds.

In our experiments the rate of dye uptake increases monotonically with laser intensity and shows weak cell-to-cell variations between 4.0×10^{12} W/cm^2 and 1.0×10^{13} W/cm^2. Above 1.0×10^{13} W/cm^2 the rate of dye uptake no longer increases with increasing laser intensities. Simultaneously, the cell-to-cell variations in dye uptake are significantly stronger. We explain this change in dye uptake by the onset of LIB in the laser focus. Since water is the main constituent of living cells, femtosecond laser-induced

TABLE I. Summary of experimentally and theoretically determined thresholds for laser-induced breakdown (LIB) in aqueous media and tissue.

Medium	Laser wavelength (nm)	Laser pulse duration (fs)	Focal spot diameter (μm)	LIB intensity threshold (W/cm^2)	LIB energy density threshold (J/cm^2)
Saline solution [18]	580	100	4.6	5.5×10^{12}	7.5
Saline solution [18]	580	400	5.3	1.3×10^{12}	9
Distilled water [21]	793	100	5.0		1.3
Human corneal tissue [14]	630	350	5.0		2
Bovine brain tissue [14]	630	100	5.0		1.5

breakdown of tissue is generally discussed by considering water as a basic model. Table I lists experimentally determined thresholds for laser-induced breakdown in various aqueous media. In addition we compare our data to experimentally determined LIB energy thresholds for soft tissue. Since laser-induced breakdown is a statistical process, experimentally determined LIB thresholds are usually defined as the 50% probability for vapor bubble formation.

The intensity threshold of 1.0×10^{13} W/cm^2 as observed in our experiment agrees well with the theoretical calculations of the LIB threshold by Kennedy *et al.* [18], Noack *et al.* [19], and experimentally determined LIB thresholds listed in Table I. The corresponding energy density threshold agrees well with the values obtained by Loesel [20] for soft tissue. As required by the definition of laser-induced breakdown we observe the statistical formation of vapor bubbles at laser intensities of 8.1×10^{12} W/cm^2 and higher. The maximum bubble diameters of 5–20 μm measured in our experiments are smaller than those measured by other authors for femtosecond laser-induced breakdown in water [21,22]. However, those experiments were performed at significantly higher laser pulse energies than our measurements.

Next, we propose a model to explain the laser intensity dependence for dye uptake by the cell. In this model we assume that laser-induced plasma formation in the laser focal spot is the origin of cell permeabilization. We start the development of the model by considering that the spatial intensity distribution in the laser focal spot is described by a Gauss function with ω_0 being the Gaussian beam waist.

$$I(r) = I_i \exp\left[-2\left(\frac{r}{\omega_0}\right)^2\right]. \tag{1}$$

The development of the model follows the recent work by Vogel *et al.* [23] who demonstrated that the spatial distribution of free electrons in the laser focus is proportional to the spatial distribution of the laser intensity. In our experiment the laser focal spot diameter ω_0 is fixed by the $\times40$ 1.3 NA microscope objective and the laser peak intensity I_i is varied by varying the incident laser power. Figure 6 illustrates how the spatial intensity distribution in the laser focal spot evolves under these experimental conditions. For a Gaussian intensity distribution the relationship between the incident laser intensity I_i and the diameter of circles of constant intensity $I_C(r_C)$ in the laser focal spot is

$$r_C^2 = \omega_0^2 \frac{1}{2} \ln\left(\frac{I_i}{I_C(r_C)}\right). \tag{2}$$

Next, we assume that the diffusive flow Φ of dye molecules into the cell is linear proportional to the size of the pore $\Phi \propto \pi r_P^2$ with $2r_P$ the diameter of the pore. The diameter of the pore is determined by the condition that for $r \leq r_P$ the laser intensity $I_i \geq I_T$ is above the required threshold for plasma creation. Using Eq. (2), we find that the flow depends on the laser intensity as

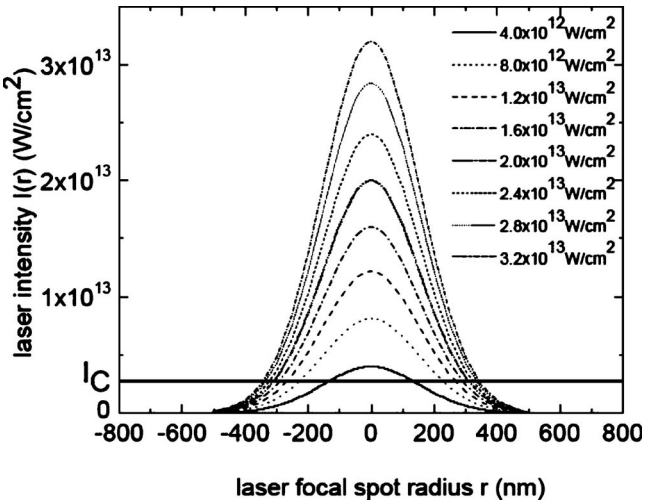

FIG. 6. Gaussian intensity distribution $I(r)$ in the laser focal spot for various laser intensities under fixed focusing conditions. The horizontal solid line indicates a line of constant intensity I_C.

$$\Phi \propto \pi r_p^2 = \omega_0^2 \frac{1}{2} \ln\left(\frac{I_i}{I_C(r_p)}\right). \quad (3)$$

A fit of this functional relationship $\Phi = A \ln(I_i/B)$ to the measured data is plotted as a solid line in Fig. 5. The fit parameters obtained are $A = 6.02 \pm 1.13$ and $B = (2.62 \pm 0.87) \times 10^{12}$ W/cm^2. The data point at $I_i = 1.2 \times 10^{13}$ W/cm^2 was excluded from the fitting procedure due to its strong deviation from the other data points. A comparison of theory and experiment reveals a good agreement for the laser intensity dependence of dye uptake by living cells under fs nir optoinjection. From this comparison we conclude that our model-based plasma formation in the laser focal spot and the Gaussian intensity distribution across the laser focal spot is a valid explanation of the rate of dye uptake by the cell in dependence of the laser intensity. In the case of a Gaussian intensity distribution across the laser focal spot, the size of the laser-induced pore increases logarithmically with increasing laser intensity under fixed focusing condition. Our experimental results and theoretical modeling also support that for laser intensities between 4.0×10^{12} W/cm^2 to 6.5×10^{12} W/cm^2, where we do not observe any indicators of LIB and only low cell-to-cell fluctuations of the rate of dye uptake for a given laser intensity, the formation of a spatially localized low-density plasma is responsible for cell membrane permeabilization. This conclusion agrees with recent numerical simulations of low density plasma effects induced by femtosecond laser pulses by Vogel *et al.* [15] and demonstrates the potential of these low density plasmas for cell manipulations on a nanometer scale. Although the cell-to-cell fluctuations of the rate of dye uptake increase significantly above the threshold for LIB, we conclude from our model that the primary origin of cell permeabilization is still the creation of a plasma in the laser focal spot and not the mechanical force due to shock wave generation and vapor bubble formation.

CONCLUSIONS

We have investigated the creation of transient pores in single living BAEC cells by fs nir laser pulses dependent on the incident laser intensity by dye uptake studies. We unambiguously demonstrate that the interaction of the laser beam with the cell membrane is the origin of pore creation. Our experimental data agree very well with the experimentally and theoretically determined thresholds for laser-induced plasma formation and LIB. We observe that pore creation is observed for laser intensities of 4.0×10^{12} W/cm^2 and higher. For laser intensities above 3.3×10^{13} W/cm^2 BAEC cells are irreversibly destroyed. Within these two limits the pore size increases logarithmically with increasing laser intensity. This functional dependence is explained by considering the Gaussian intensity distribution across the laser focal spot. The physical understanding of the relationship between pore size and laser intensity allows the control of the number of molecules delivered into a cell per unit time through the control of the pore size. Our results provide strong experimental evidence that the theory of laser-induced plasma formation is a valid description of femtosecond near-infrared optoinjection in living mammalian cells. We would like to point out that any prior experimental work on the mechanisms of femtosecond laser nanosurgery in cell biology was restricted to the study of laser plasma formation in aqueous solutions or the determination of laser ablation width in fixed (dead) cells.

ACKNOWLEDGMENTS

We acknowledge fruitful discussions and technical support by I. Giaever and C. Keese, and both Rensselaer Polytechnic Institute and Applied Biophysics Inc. The authors also thank Chunzhi Dong for his technical assistance.

[1] I. Hapala, Crit. Rev. Biotechnol. **17**, 105 (1997).
[2] O. Feinerman and E. Moses, J. Neurosci. Methods **127**, 75 (2003).
[3] S. Orlowski and M. Liuis, Biochim. Biophys. Acta **1154**, 51 (1993).
[4] T. Y. Tsong, Biophys. J. **60**, 297 (1991).
[5] J. E. Biewenga, O. H. J. Destree, and L. H. Schrama, J. Neurosci. Methods **71**, 67 (1997).
[6] W. Tao, J. Wilkinson, E. Stanbridge, and M. W. Berns, Proc. Natl. Acad. Sci. U.S.A. **84**, 4180 (1987).
[7] G. Palumbo, M. Caruso, E. Crescenzi, M. F. Tecce, G. Roberti, and A. Colasanti, J. Photochem. Photobiol., B **36**, 41 (1996).
[8] H. Schneckenburger, A. Hendinger, R. Sailer, W. S. Strauss, and M. Schmidt, J. Biomed. Opt. **7**, 410 (2002).
[9] L. Paterson, B. Agate, M. Comrie, R. Ferguson, T. K. Lake, J. E. Morris, A. E. Carruthers, C. T. A. Brown, W. Sibbett, P. E. Bryant, F. Gunn-Moore, A. C. Riches, and K. Dholakia, Opt. Express **13**, 595 (2005).
[10] Y. Shirahata, N. Ohkohchi, H. Itagak, and S. Satomi, J. Investig. Med. **49**, 184 (2001).
[11] U. K. Tirlapur and K. Koenig, Nature (London) **418**, 290 (2002).
[12] S. K. Mohanty, M. Sharma, and P. K. Gupta, Biotechnol. Lett. **25**, 895 (2003).
[13] K. Koenig, J. Microsc. **200**, 83 (2000).
[14] M. H. Niemz, *Laser-Tissue Interactions—Fundamentals and Applications* (Spinger, Berlin, 2004).
[15] A. Vogel, J. Noack, G. Huttmann, and G. Paltauf, Proc. SPIE **4620**, 202 (2002).
[16] A. Heisterkamp, I. Z. Maxwell, and E. Mazur, Opt. Express **13**, 3690 (2005).
[17] F. H. Loesel, J. P. Fischer, M. H. Gotz, C. Horvath, T. Juhasz, F. Noack, N. Suhm, and J. F. Bille, Appl. Phys. B: Lasers Opt. **66**, 121 (1998).
[18] P. K. Kennedy, D. X. Hammer, and B. A. Rockwell, Prog. Quantum Electron. **21**, 155 (1997).
[19] J. Noack and A. Vogel, IEEE J. Quantum Electron. **35**, 1156 (1999).

[20] F. H. Loesel, M. H. Niemz, J. F. Bille, and T. Juhasz, IEEE J. Quantum Electron. **32**, 1717 (1996).

[21] S. M. Milas, J. Y. Ye, T. B. Norris, K. W. Hollman, S. Y. Emelianov, and M. O'Donnell, IEEE Trans. Ultrason. Ferroelectr. Freq. Control **50**, 517 (2003).

[22] E. N. Glezer, C. B. Schaffer, N. Nishmura, and E. Mazur, Opt. Lett. **22**, 1817 (1997).

[23] A. Vogel, J. Noack, G. Huettmann, and G. Paltauf, Appl. Phys. B: Lasers Opt. **81**, 1015 (2005).

[24] The laser focal spot radius r_L is calculated using geometrical optics and Abbe's theory of the resolution of a microscope. In comparison the on-axis intensity of a Gaussian beam $I(0) = 2P/(\pi\omega_0^2)$ with ω_0 being the Gaussian beam waist in the laser focal spot.